AIAA 81-0146R

Remote Control Canard Missile with a Free-Rolling Tail Brake Torque System

A.B. Blair Jr.*
NASA Langley Research Center, Hampton, Va.

An experimental wind-tunnel investigation has been conducted at supersonic Mach numbers to determine the static aerodynamic characteristics of a cruciform canard-controlled missile with fixed and free-rolling tail-fin afterbodies. Mechanical coupling effects of the free-rolling tail afterbody were investigated using an electronic/electromagnetic brake system that provides arbitrary tail-fin brake torques with continuous measurements of tail-to-mainframe torque and tail-roll rate. Results are summarized that show the free-rolling tail configuration reduced and linearized induced rolling moments due to canard yaw control and eliminated canard roll control reversals that are typical for the fixed-tail configuration. Data are presented that allow compromises to be made in bearing friction which results in satisfactory free-tail aerodynamic characteristics that include reductions in adverse rolling moments and lower tail-fin spin rates.

Nomenclature

A = reference area; maximum cross-sectional area of model body, $\pi d^2/4$
C_A = axial-force coefficient, axial force/qA
C_l = rolling moment coefficient, rolling-moment/qAd
C_m = pitching moment coefficient, pitching moment/qAd
C_N = normal-force coefficient, normal force/qA
C_n = yawing-moment coefficient, yawing moment/qAd
C_Y = side-force coefficient, side force/qA
d = reference diameter
M = Mach number
q = freestream dynamic pressure
α = angle of attack
δ_{pitch} = pitch-control deflection of two canards; positive for leading-edge up, deg
δ_{roll} = differential deflections of pitch canards, individual canards are deflected indicated amount; positive to provide clockwise rotation when viewed from rear, deg
δ_{yaw} = yaw-control deflection of two canards; positive for leading-edge right when viewed from rear, deg
ϕ_c = model roll angle; positive clockwise when viewed from rear ($\phi_c = 0$ deg, canards are in vertical and horizontal planes), deg
$\dot{\phi}_{tail}$ = roll rate of tail-fin afterbody; positive clockwise when viewed from rear, rpm

Model Configuration Designation

FIXED = tail-fin afterbody locked (no rotation)
FREE = tail-fin afterbody free (no brake friction torque)
+ = tail fins locked inline with canards
× = tail fins locked interdigitated with canards

Introduction

IT is well documented that missile configurations utilizing forward surfaces to provide control experience the problem of induced rolling moments at supersonic Mach numbers. For these forward-controlled configurations, the need is either that of reducing or eliminating the induced rolling moments or that of providing an efficient system for their control.

One approach that is suggested in Ref. 1 uses the free-rolling tail concept to reduce adverse rolling moments on a canard-controlled missile. A free-rolling tail reduces the rolling moments by uncoupling the tail from the missile airframe and also allows canard roll control at low angles of attack. The free-rolling tail concept gives canard-controlled missiles more simplicity and modular flexibility by having a single cruciform canard control system that provides pitch, yaw, and roll control.

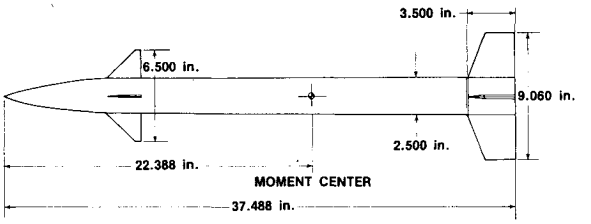

Fig. 1 Model details.

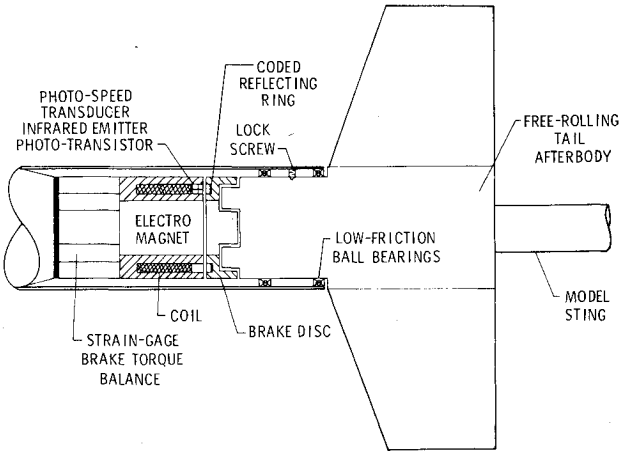

Fig. 2 Electronic/electromagnetic brake system.

Presented as Paper 81-0146 at the AIAA 19th Aerospace Sciences Meeting, St. Louis, Mo., Jan. 12-15, 1981; submitted March 6, 1981; revision received July 13, 1981. This paper is declared a work of the U.S. Government and therefore is in the public domain.

*Aero-Space Technologist, Supersonic Aerodynamics Branch, High-Speed Aerodynamics Division. Member AIAA.

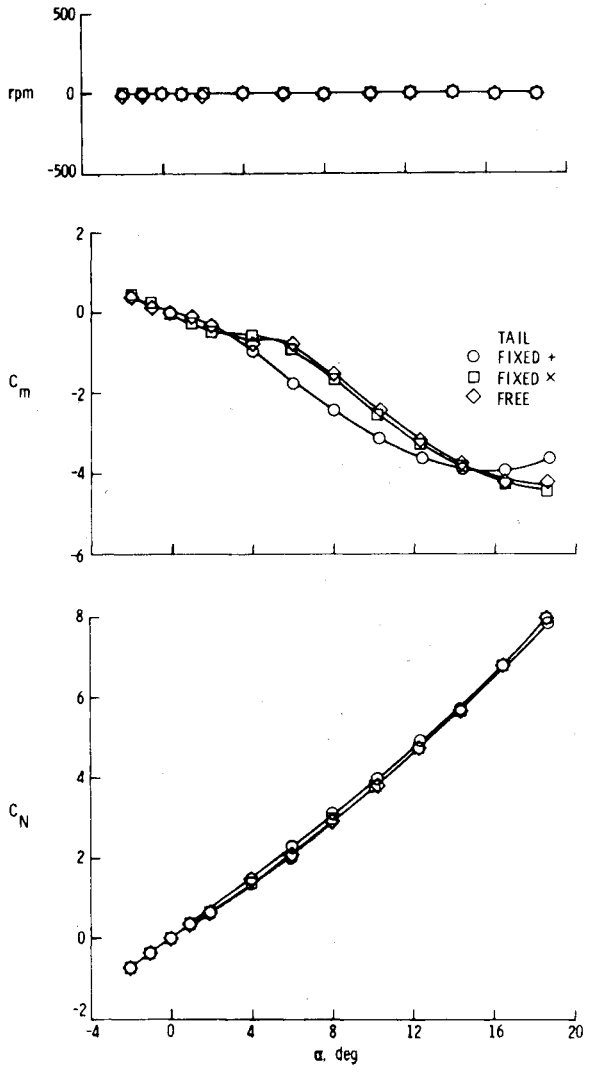

Fig. 3 Effect of fixed and free-rolling tail on longitudinal characteristics. $M = 1.70$; $\phi_c = 0$ deg; zero canard deflection.

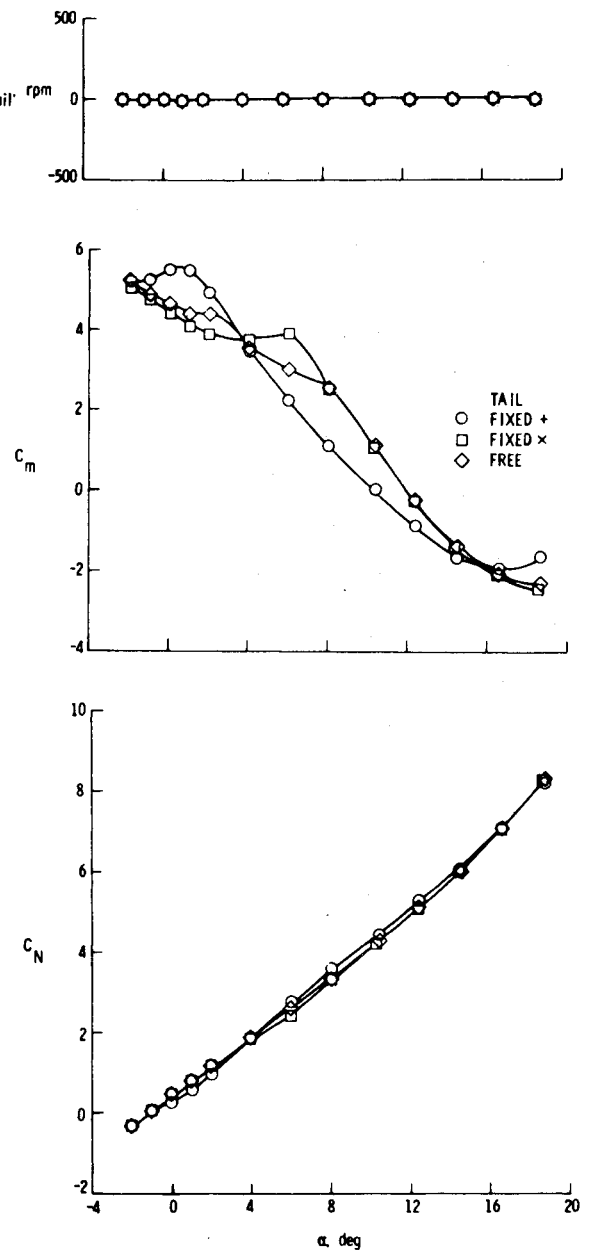

Fig. 4 Effect of fixed and free-rolling tail on pitch control characteristics. $M = 1.70$; $\phi_c = 0$ deg; $\delta_{pitch} = 10$ deg.

The idea of using free-rolling tail fins is not new. From 1950 to 1960, NASA and its predecessor, NACA, investigated a number of roll-control devices in free flight as part of their aerodynamic control research program for missiles and airplanes. For some of these tests a free-rolling tail-fin assembly was used on the missile airframes, not only to provide the models with longitudinal and directional stability, but also to eliminate unwanted induced rolling moments that were generated by the various roll controls under investigation.[2] In many cases, the free-rolling tails were on nonmaneuvering missile systems (e.g., boost-glide trajectories at low angles of attack). More recently, the U.S. Navy has conducted research[3-5] using the rolling tail concept on free-fall stores and missiles.

This paper summarizes the significant findings of an experimental wind-tunnel investigation whose purpose was to extend the fixed and free-tail aerodynamic data base of Ref. 6 by studying the mechanical coupling effects of a free-rolling tail afterbody on a canard-controlled missile with pitch, yaw, and roll control.

Model Concept and Tests

The research model was a cruciform missile configuration that consisted of a remote control canard forebody interfaced with a free-rolling tail afterbody incorporating an electronic/electromagnetic braking system. Overall dimensions of the model are shown in Fig. 1.

The remote control canards were the primary method for inducing tail-fin rotation since the tail fins were not canted. Remote control canards provide a more selective and precise control of the canard-generated flowfields produced by the various deflections for pitch, yaw, and roll control. Many of these canard flowfields produce tail-flow environments that will spin a free-to-roll tail afterbody.

The electronic/electromagnetic brake system provides arbitrary tail-fin brake torques with continuous measurements of tail-to-mainframe torque and tail-roll rate. A sketch of this system is shown in Fig. 2. The free-tail afterbody is mounted on a set of low-friction ball bearings and is coupled to an electromagnet by a free-floating torque brake disk which makes up part of the magnetic path. The brake disk is held to the electromagnet with a force proportional to a command current with the friction between them producing the desired torque. Each sliding surface has a nonmagnetic hard surface coating to reduce wear and produce a magnetic gap to remove residual magnetism when the current goes to zero. The electromagnet is mounted to a one-component

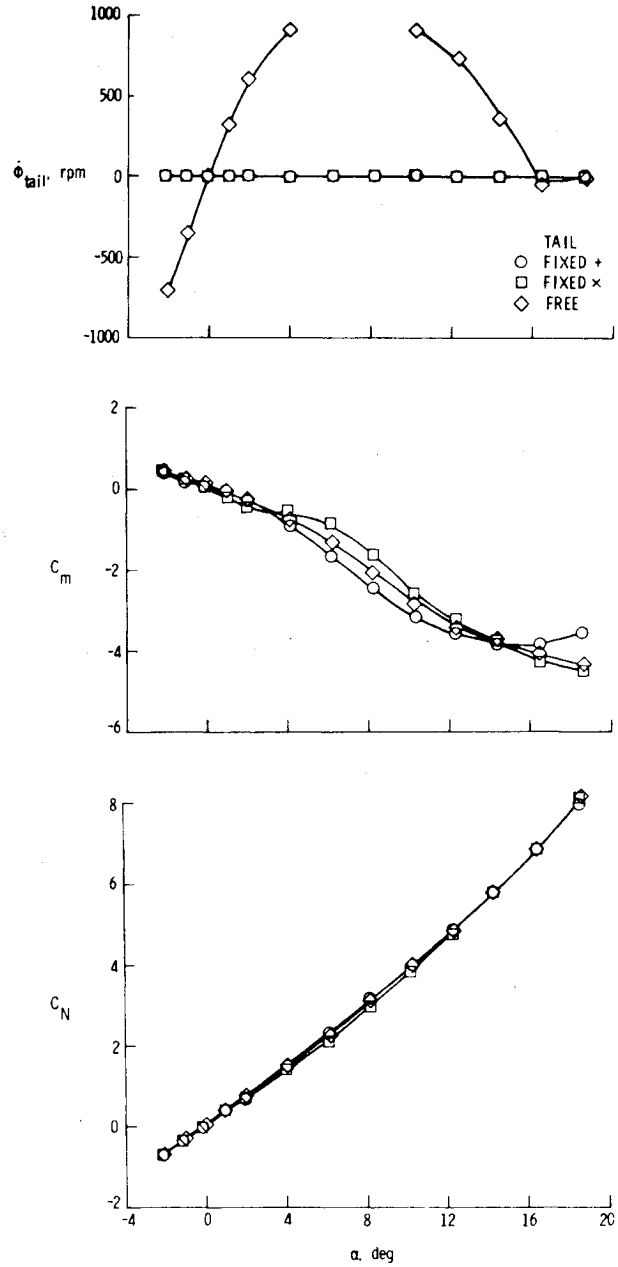

Fig. 5 Effect of fixed and free-rolling tail on longitudinal characteristics. $M = 1.70$; $\phi_c = 0$ deg; $\delta_{yaw} = -10$ deg.

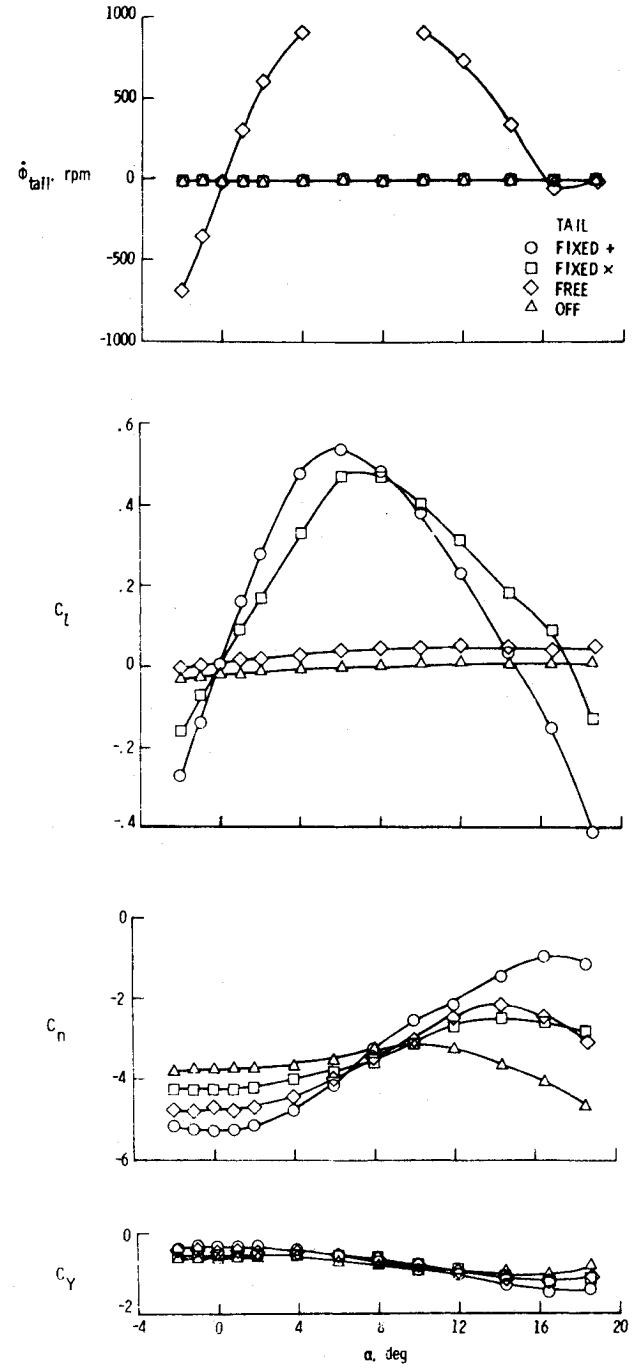

Fig. 6 Effect of fixed and free-rolling tail on lateral-directional characteristics. $M = 1.70$; $\phi_c = 0$ deg; $\delta_{yaw} = -10$ deg.

strain-gage torque balance that measures tail brake reaction torques while the tail is rotating in either direction. The electromagnet can provide command brake torque absolute values from 0 to 6 in.-lb and is capable of holding selected values for various tail-flow conditions using feedback control from the brake torque balance in combination with electronic servo amplifier circuits. For fixed-tail configurations the tail-fin afterbody can be locked inline, "+" position or interdigitated, "×" position with the canards using a lock screw.

Tail-fin roll rates are measured by a photospeed transducer composed of an infrared emitter and phototransistor mounted in the electromagnet coil slot. A coded reflecting ring is mounted on the brake disk to reflect pulses of light from the infrared emitter to the phototransistor which converts them to electrical pulses to obtain tail-fin roll rate. The roll rates are nominally limited to ±1000 rpm as a safety precaution with an accuracy of ±25 rpm.

By using the electronic/electromagnetic braking system, several simulated bearing friction torques (mechanical coupling effects) can be evaluated with respect to their effects on missile aerodynamics and results can be presented along with the fixed and free-tail (no brake friction) data. Perhaps there is a compromise on bearing friction, e.g., low-cost bearings with some friction, that will allow satisfactory aerodynamic stability and control characteristics while reducing adverse induced roll effects and maintaining low tail-fin spin rates.

The tests were conducted in the Langley Unitary Plan Wind Tunnel at Mach numbers from 1.70 to 2.86. The nominal angle-of-attack range was −4 to 18 deg at a model (canard) roll angle of 0 deg and at a Reynolds number of 6.6×10^6/m (2.0×10^6/ft). A six-component strain-gage balance was used to measure the aerodynamic forces and moments on the model. All tests were performed with boundary-layer transition strips on both sides of the canards and tail fins and aft of the model nose.

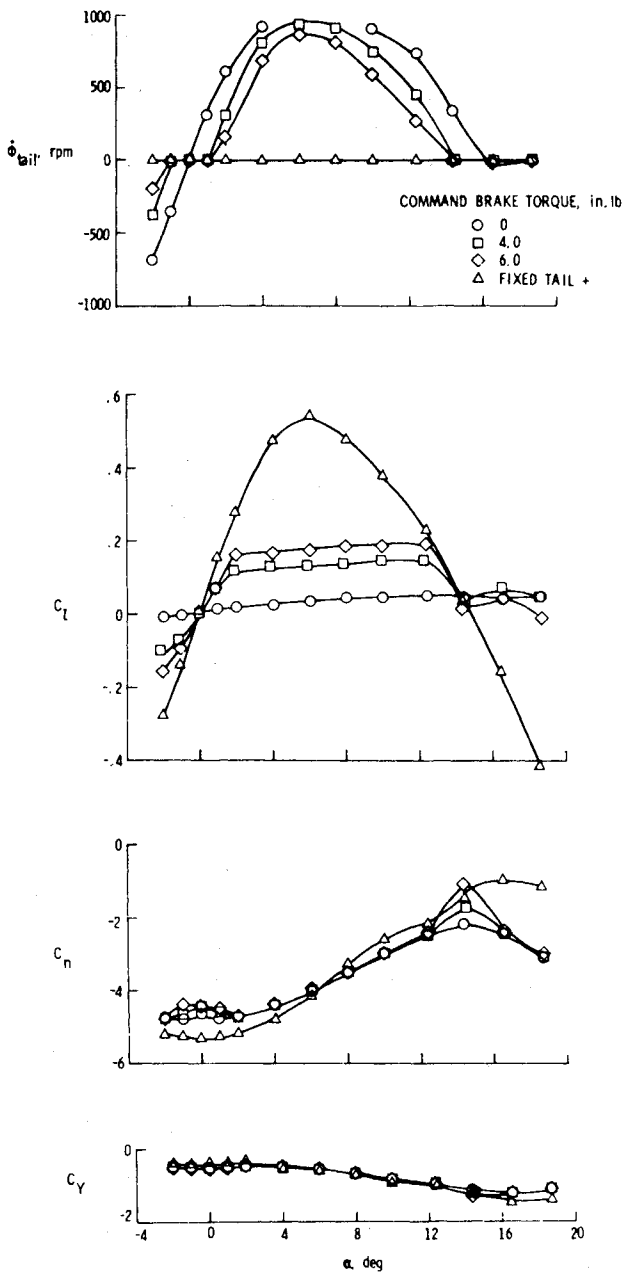

Fig. 7 Effect of command brake torque on free-rolling tail lateral-directional characteristics. $M = 1.70$; $\phi_c = 0$ deg; $\delta_{yaw} = -10$ deg.

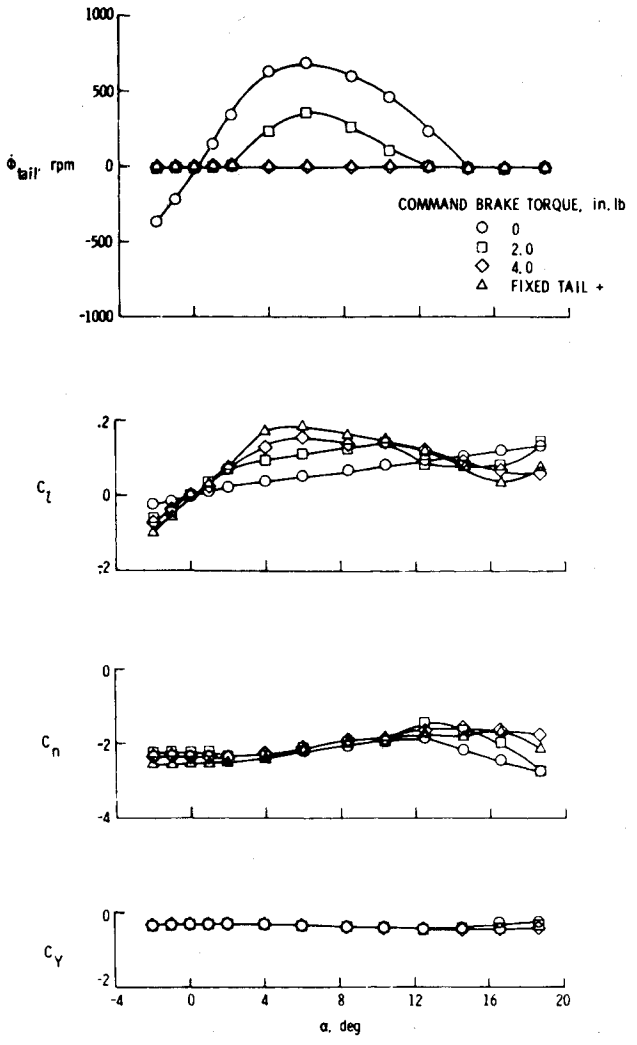

Fig. 8 Effect of command brake torque on free-rolling tail lateral-directional characteristics. $M = 2.86$; $\phi_c = 0$ deg; $\delta_{yaw} = -10$ deg.

Results and Discussion

The effect of fixed and free-rolling tail fins on the longitudinal aerodynamic characteristics of the model with zero control deflection is presented in Fig. 3. To make a more meaningful comparison with the free-tail configurations, all fixed-tail data are presented with the tail fins in both the inline, "+" position and interdigitated "×" position with respect to the canards at $\phi_c = 0$ deg. The remote control canards allow precise zero canard settings such that a uniform flowfield can be created with no significant asymmetric flow conditions at the tail. Under these conditions, the tail fins (no fin cant) have a preferred orientation with only small oscillation angles usually interdigitated with the canards for $\phi_c = 0$ deg. For example, this type of tail flowfield is verified by a zero tail-fin spin rate. The pitch characteristics of the free-tail configuration, in general, exhibit the same trends as the fixed-interdigitated tail configuration which are characterized by pitch up that coincides with loss of normal force coefficient.

Pitch control characteristics for the fixed and free-tail configurations are presented in Fig. 4. The canard pitch control generates a strong symmetrical downwash flowfield which for the fixed-inline tail configuration contributes to pitch up near $\alpha = 0$ deg. The fixed-interdigitated and free-tail configurations have similar pitch characteristics; however, for the free-tail configuration, pitch up is reduced and occurs at lower angles of attack.

The longitudinal and lateral-directional aerodynamic characteristics of the fixed and free-tail configurations with a canard yaw control are presented in Figs. 5 and 6, respectively. The yaw control generates a tail-flow environment that produces changes in tail-fin roll rate magnitude and spin direction at low to moderate angles of attack. In general, for the free-tail configuration (Fig. 5) the pitching-moment data are more linear and fall between that of the fixed-tail configurations. For the fixed-tail configuration in Fig. 6, the data show the usual induced rolling-moment coefficients that are typical for a canard yaw control. These coefficients are reduced and linearized for the free-tail configuration. In general, the level of yaw control of the free-tail configuration is between the fixed-tail configurations at low to moderate angles of attack. The effect of command brake torque values on the lateral-directional aerodynamic characteristics of the free-tail configuration with a yaw control is presented in Figs. 7 and 8. These brake torque values simulated absolute increments of bearing friction torques. In these figures, the data show that increases in simulated bearing friction raises the

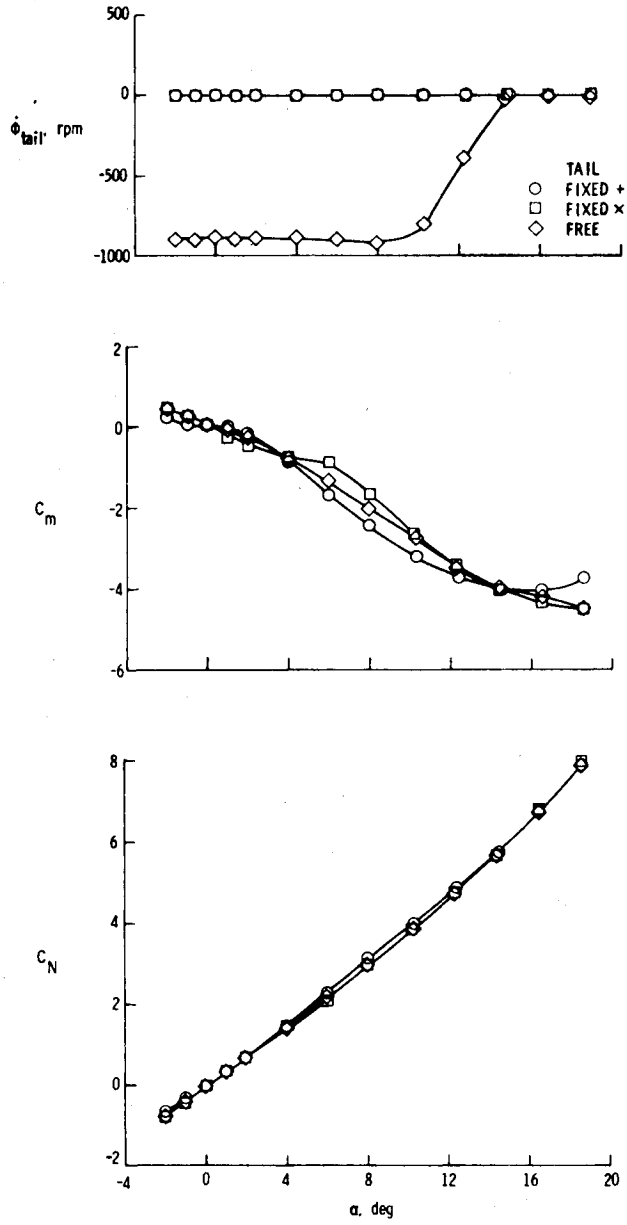

Fig. 9 Effect of fixed and free-rolling tail on longitudinal characteristics. $M = 1.70$; $\phi_c = 0$ deg; $\delta_{roll} = 5$ deg.

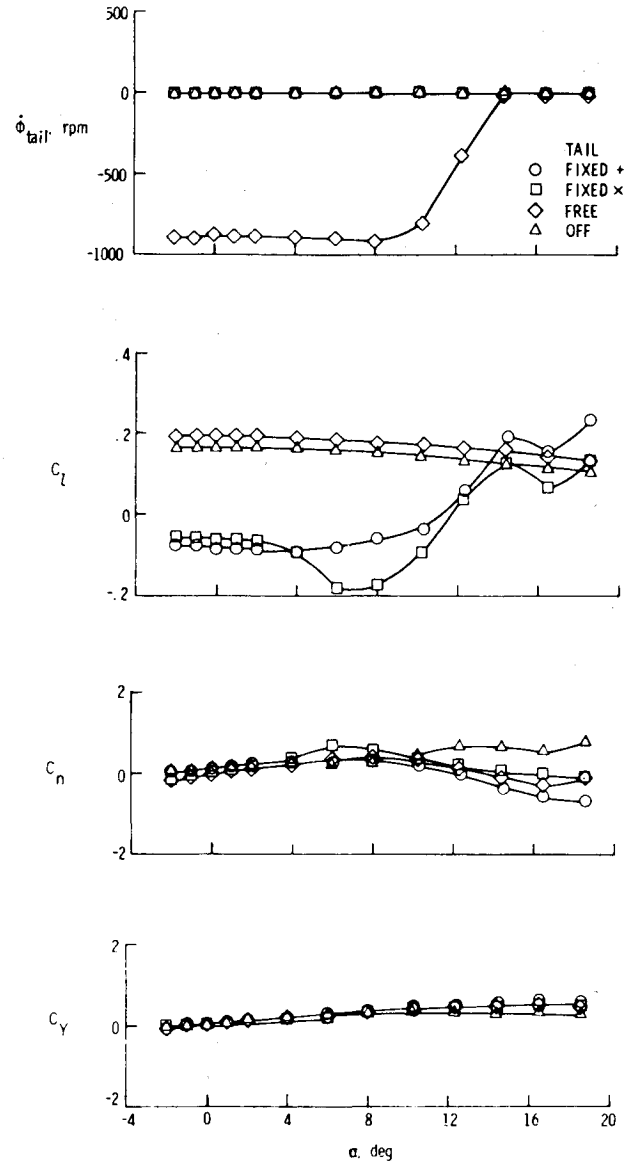

Fig. 10 Effect of fixed and free-rolling tail on lateral-directional characteristics. $M = 1.70$; $\phi_c = 0$ deg; $\delta_{roll} = 5$ deg.

level of induced rolling-moment coefficient in a linear manner toward fixed-tail values, while yaw control remains about the same. Of course, there are reductions in tail-fin roll rates with increases in simulated bearing friction and for $M = 2.86$ (Fig. 8) the tail fin rotation is stopped. It appears that a compromise on bearing friction, e.g., low-cost bearings with some friction, may allow satisfactory yaw-control characteristics with low tail spin rates while reducing adverse rolling moments.

The longitudinal and lateral-directional aerodynamic characteristics of the fixed and free-tail configurations with a canard roll control are presented in Figs. 9 and 10, respectively. The canard roll control produces a strong asymmetrical flowfield at the tail fins which is demonstrated by the steady-state roll rates of the tail fins at low to moderate angles of attack. For these tail-flow conditions the pitch trends (Fig. 9) of the free-tail configuration are similar to those of the fixed-interdigitated tail configuration except at intermediate angles of attack where it is between the fixed-tail configurations. In Fig. 10, the data of the fixed-tail configurations illustrate typical canard roll control reversals at low angles of attack. The canards of the free-rolling tail configuration provide conventional roll control in the low to moderate angle-of-attack range. This roll control is reduced with increases in absolute brake torque values that are presented in Figs. 11 and 12.

Conclusions

The results of this study indicate, for zero control deflection, the pitching-moment characteristics of the free-tail configuration generally follow the same trends as those of the fixed-interdigitated tail configuration. The free-rolling tail configuration reduced and linearized induced rolling moments due to canard yaw control and eliminated canard roll control reversals that are typical for the fixed-tail configurations. The canards of the free-tail configuration provide conventional roll control in the low to moderate angle-of-attack range. For the free-tail configuration with increases in brake torque, which simulated bearing friction torque, the induced roll due to yaw control increased and the canard roll control decreased. Data are presented that allow compromises to be made in bearing friction which result in satisfactory free-tail aerodynamic characteristics that include reductions in adverse rolling moments and lower tail-fin spin rates.

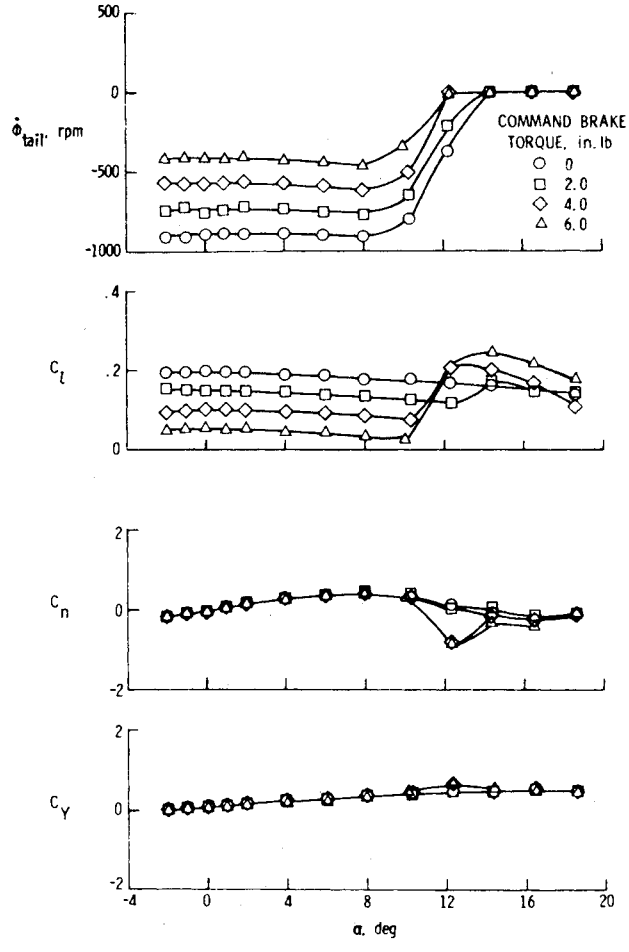

Fig. 11 Effect of command brake torque on free-rolling tail lateral-directional characteristics. $M = 1.70$; $\phi_c = 0$; $\delta_{roll} = 5$ deg.

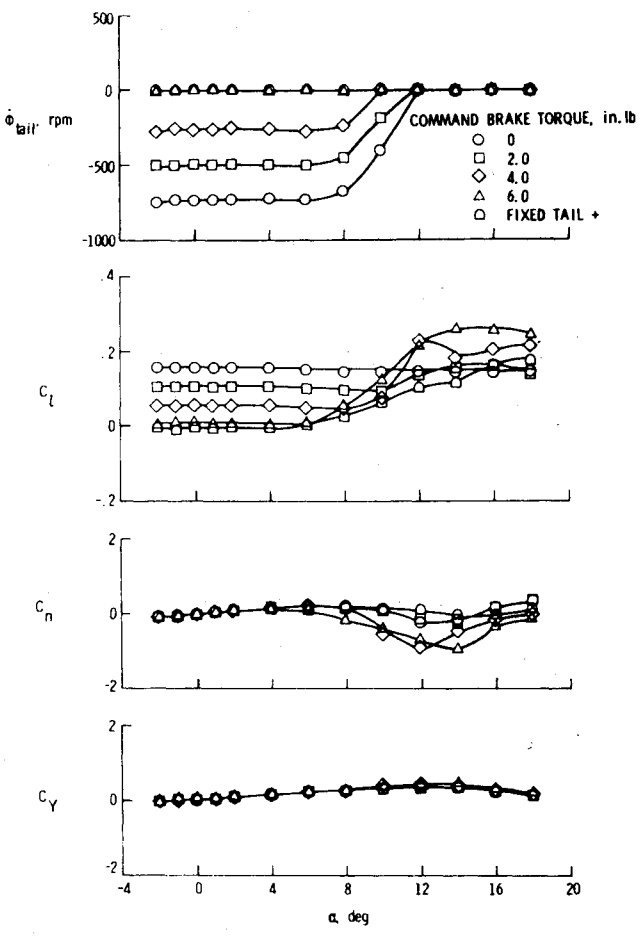

Fig. 12 Effect of command brake torque on free-rolling tail lateral-directional characteristics. $M = 2.16$; $\phi_c = 0$ deg; $\delta_{roll} = 5$ deg.

Acknowledgments

The author would like to express a debt of gratitude and his appreciation to William T. Davis and David C. Davis of NASA Langley Research Center for their technical support in the design, construction, and evaluation of the electronic systems used in the research model.

References

[1]Sawyer, W.C., Jackson, C.M. Jr., and Blair, A.B. Jr., "Aerodynamic Technologies for the Next Generation of Missiles," AIAA paper presented at the AIAA/ADPA Tactical Missile Conference, Gaithersburg, Md., April 1977.

[2]Schult, E.D., "Free-Flight Measurements of the Rolling Effectiveness and Operating Characteristics of a Bellows-Actuated Split-Flap Aileron on a 60° Delta Wing at Mach Numbers Between 0.8 and 1.8," NACA RM L54H17, Oct. 1954.

[3]Regan, F.J. and Falusi, M.E., "The Static and Magnus Aerodynamic Characteristics of the M823 Research Store Equipped with Fixed and Freely Spinning Stabilizers," U.S. Navy, NOLTR 72-291, Dec. 1972. (Available from DDC as AD 757 658.)

[4]Regan, F.J., Shannon, J.H.W., and Tanner, F.J., "The Joint N.O.L./R.A.E./W.R.E. Research Programme on Bomb Dynamics. Part III. A Low-Drag Bomb with Freely Spinning Stabilizers," Australian Def. Sci., Serv., WRE-Report-904 (WR&D), June 1973.

[5]Darling, J.A., "Elimination of the Induced Roll of a Canard Control Configuration by Use of a Freely Spinning Tail," U.S. Navy, NOLTR 72-197, Aug. 1972.

[6]Blair, A.B. Jr., "Wind-Tunnel Investigation at Supersonic Speeds of a Canard-Controlled Missile with Fixed and Free-Rolling Tail Fins," NASA TP-1316, Sept. 1978.